SECOND ORDER PYRAMIDAL SLIP IN ZINC SINGLE CRYSTALS

K. H. Adams,* R. C. Blish and T. Vreeland, Jr.
W. M. Keck Laboratory of Engineering Materials
California Institute of Technology
Pasadena, California (U.S.A.)

ABSTRACT

Measurements of strain, dislocation mobility and dislocation density have been made in 99.999% zinc single crystals stressed at room temperature in compression along the hexagonal axis, [0001]. Slip bands on the $\langle 1\bar{2}1\bar{3} \rangle$ { $1\bar{2}12$ }, second order pyramidal system were observed. Etch pit observations indicate that the average dislocation density increases linearly with strain. The velocity of edge dislocations in slip bands obeys the relation $v = v_o(\tau/\tau_o)^n$ with $v_o = 1$ in/sec, $n = 8.7$, $\tau_o = 870$ lb/in^2, and τ the resolved shear stress in lb/in^2. These observations together with measurements of the strain-rate sensitivity of the flow stress show that the stress dependence of the density of moving dislocations is more important than the stress dependence of the dislocation velocity as they affect the strain-rate sensitivity.

INTRODUCTION

The stress dependence of the mobility of basal dislocations in zinc single crystals has recently been reported by Adams et al. [1]. The same experimental techniques have been applied in a study of the $\langle 1\bar{2}1\bar{3} \rangle$ { $1\bar{2}12$ }, second order pyramidal slip system. The $\langle 1\bar{2}1\bar{3} \rangle$ { $1\bar{2}12$ } slip system was originally confirmed as a nonbasal slip system in zinc

---

*Present Address: Department of Mechanical Engineering, Tulane University, New Orleans, La. (U.S.A.).

by Rosenbaum [2] from etch pit and slip line observations. Additional supporting evidence has been provided by Price [3] from electron microscope observations of the formation and climb of dislocation loops in the $\langle 1\bar{2}1\bar{3} \rangle$ { $1\bar{2}12$ } slip system. Predvoditelev et al. [4] demonstrated that extensive slip takes place at room temperature on the $\langle 1\bar{2}1\bar{3} \rangle$ { $1\bar{2}12$ } system in zinc as a result of concentrated loads applied normal to a (0001) surface. Some twinning and slip on first order pyramidal planes was observed, but the second order pyramidal slip was considerably more extensive. Lavrent'yev et al. [5] measured the stress required to start slip bands on the second order pyramidal slip system in zinc. They reported that this stress increases markedly with an increase in substructure, and also with a decrease in temperature.

The importance of nonbasal slip in zinc in determining the flow stress for basal slip has been clearly demonstrated by Stofel and Wood [6] in combined tension and torsion tests about the [0001] direction. Studies of the effect of impurity additions on the basal flow stress have also suggested the importance of nonbasal dislocation densities [7].

The present investigation was undertaken to obtain a better understanding of the character and dynamics of second order pyramidal slip in zinc. Results are presented on the direct determination of dislocation mobility by etch pit observations, the increase in dislocation density with strain and the strain-rate sensitivity of the flow stress.

EXPERIMENTAL PROCEDURE

Single crystals were prepared from C.P. grade zinc of 99.999% purity obtained from the New Jersey Zinc Company. Single crystals test specimens were oriented and prepared by spark erosion and acid cutting techniques described previously [1, 8]. The compression test specimens used were in the form of 1/2 inch cubes oriented with two (0001) loading surfaces, two $(10\bar{1}0)$ surfaces suitable for dislocation etching and two $(\bar{1}2\bar{1}0)$ surfaces. Several cylindrical compression specimens, 3/8 inch diameter and 1 inch long, with a [0001] cylindrical axis were prepared and used for stress-strain and dislocation density vs. strain measurements. All specimens were annealed prior to testing at 700°F in a purified hydrogen atmosphere for 4 to 8 hrs.

Stress-strain and strain-rate sensitivity tests were carried out in an Instron testing machine. Strain was measured with two type FAP-25-12 foil strain gages obtained from the Baldwin-Lima-Hamilton Corporation. The gages were bonded to opposite sides of the specimens using SR-4 cement and two dummy gages were mounted on an unstressed specimen to complete a Wheatstone bridge circuit. Stress-strain tests were carried out at a crosshead speed of 0.001 in/min. For stress-strain tests the compressive load and stain were recorded on an X-Y

recorder. Strain-rate sensitivity was determined by suddenly changing the crosshead speed from 2×10^{-3} in/min to 2×10^{-4} in/min and from 2×10^{-4} in/min to zero. Load and strain were recorded vs. time on a Consolidated Electrodynamics oscillograph in the strain-rate sensitivity tests.

Compression load pulses were applied to the cube type specimens in a rapid load testing machine to determine dislocation mobility. The $(10\bar{1}0)$ surfaces of the specimen were etched and replicated before and after testing. Re-etching was accomplished within 3 min after application of a load pulse. Replicas were flashed with aluminum for optical examination. Etching and replication were likewise carried out during stress-strain tests to determine the change in dislocation density with increasing strain.

EXPERIMENTAL RESULTS

A typical room temperature stress-strain curve is shown in Fig. 1. The curve shows relatively rapid work hardening after the elastic limit is exceeded. Typical areas of the replicas obtained from strained and etched specimens are shown in Fig. 2 for several different levels of strain. An area which exhibits pyramidal slip plane traces of all six

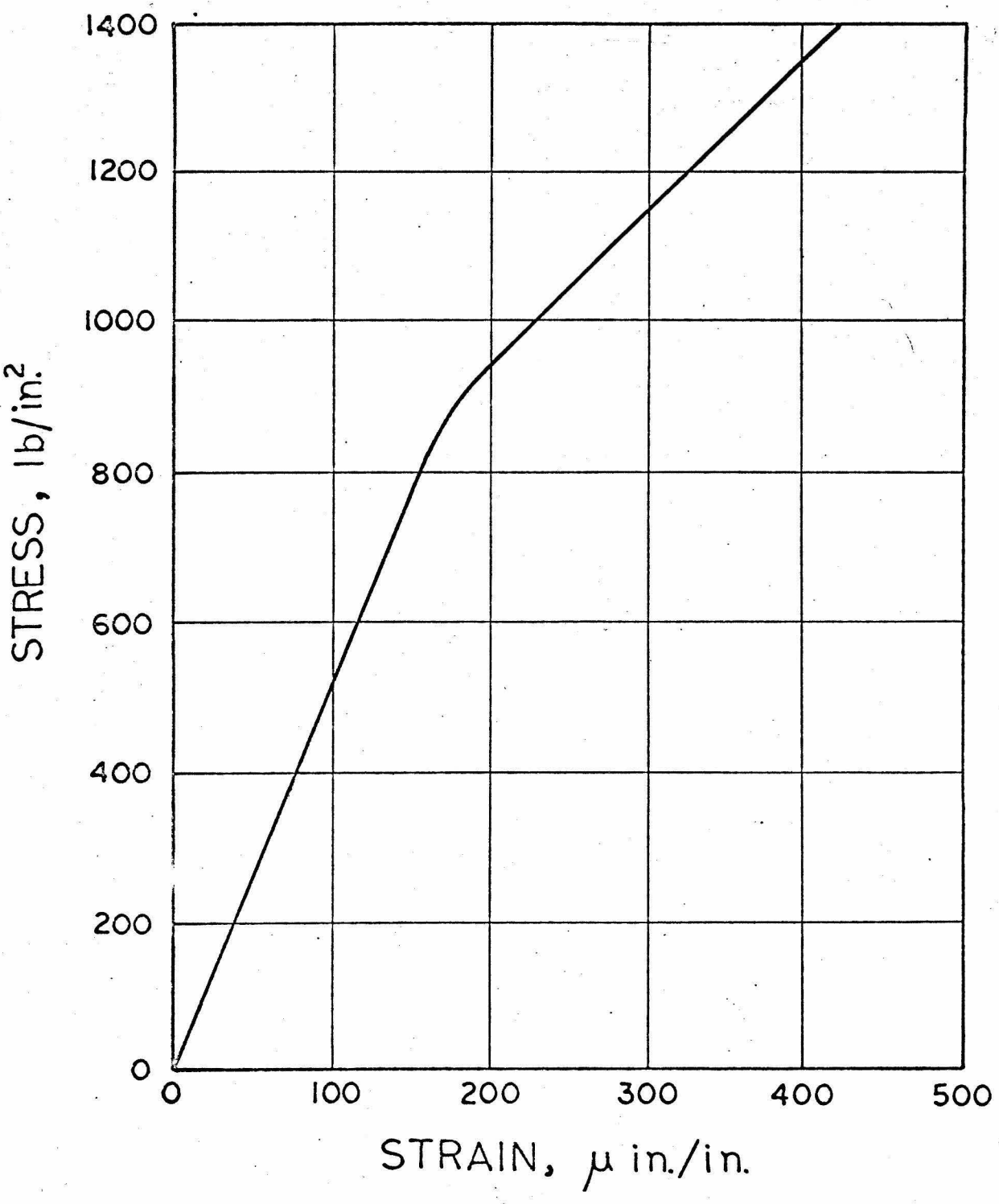

Fig. 1 Compressive stress vs. compressive strain along [0001], 99.999% zinc at room temperature.

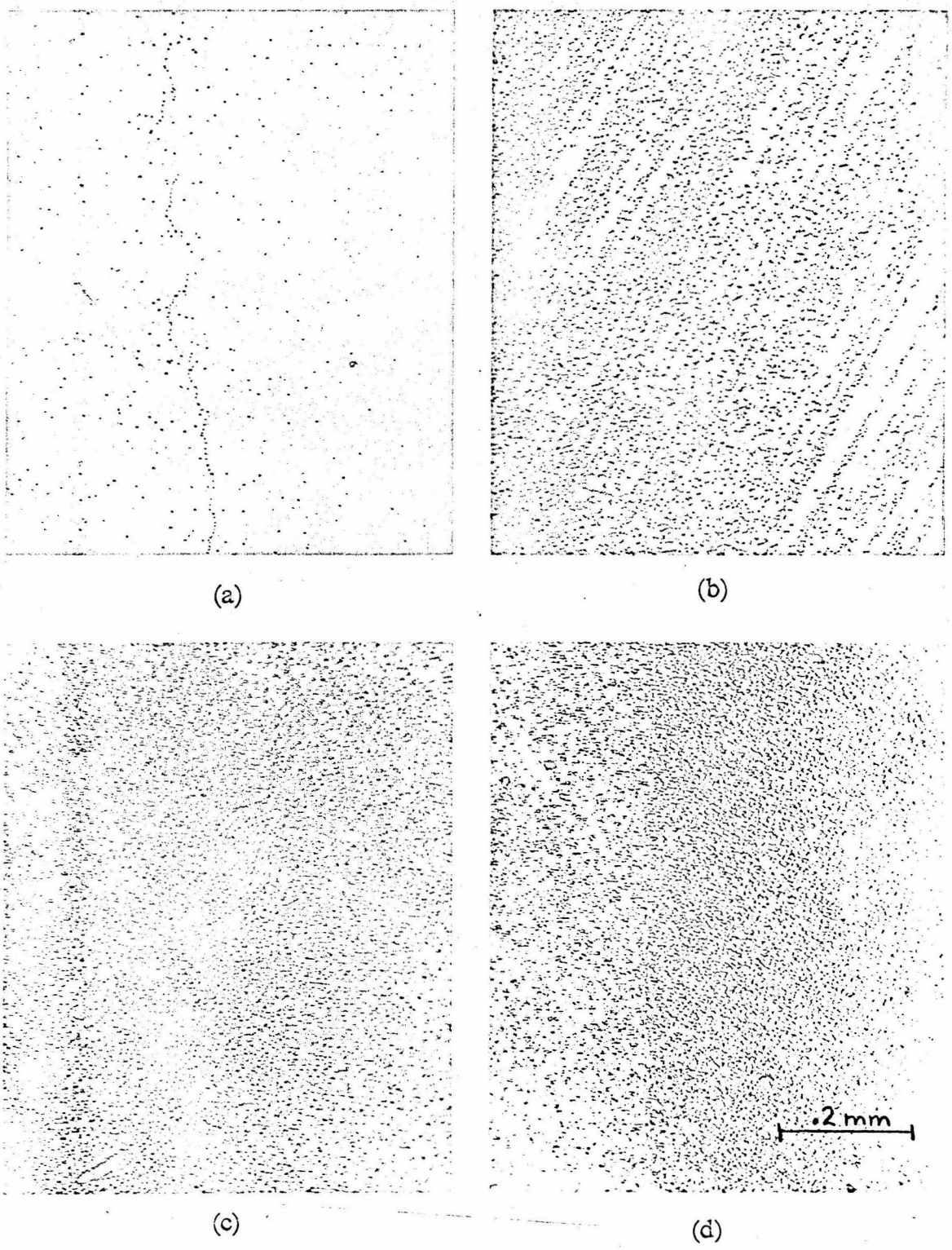

Fig. 2 Typical areas of specimens strained in compression along [0001], $(10\bar{1}0)$ surface. (a) No strain, (b) 132 μ in/in, (c) 270 μ in/in, (d) 395 μ in/in. Lines indicate $[\bar{1}2\bar{1}0]$ direction, compression axis is vertical.

different slip systems is shown in Fig. 3. The etch pit density as a function of compressive strain along the [0001] axis is shown in Fig. 4. The bars associated with each point indicate the range of densities observed over different areas on the $(10\bar{1}0)$ surfaces and the points represent the mean value of the etch pit counts made at a given strain level.

The strain-rate sensitivity of the flow stress for second order pyramidal slip was found to be considerably less than the value previously reported for the basal system [1]. Very small stress jumps accompany a sudden change in strain-rate. The inverse strain-rate sensitivity is defined as

$$n' = \frac{\partial \ln \dot{\gamma}_p}{\partial \ln \tau}$$

or

$$n' \cong \frac{\ln (\dot{\gamma}_{p_2} / \dot{\gamma}_{p_1})}{\Delta\tau/\tau} \qquad (1)$$

where $\dot{\gamma}_{p_2}$ is the plastic strain-rate after the change, $\dot{\gamma}_{p_1}$ is the plastic strain-rate before the change and $\Delta\tau$ is the jump in resolved

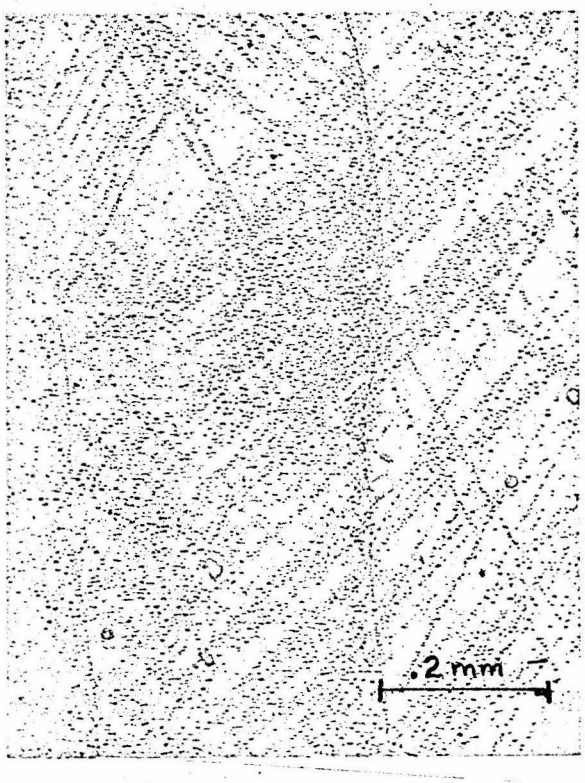

Fig. 3 An area showing slip bands on the six systems intersecting the $(10\bar{1}0)$ plane.

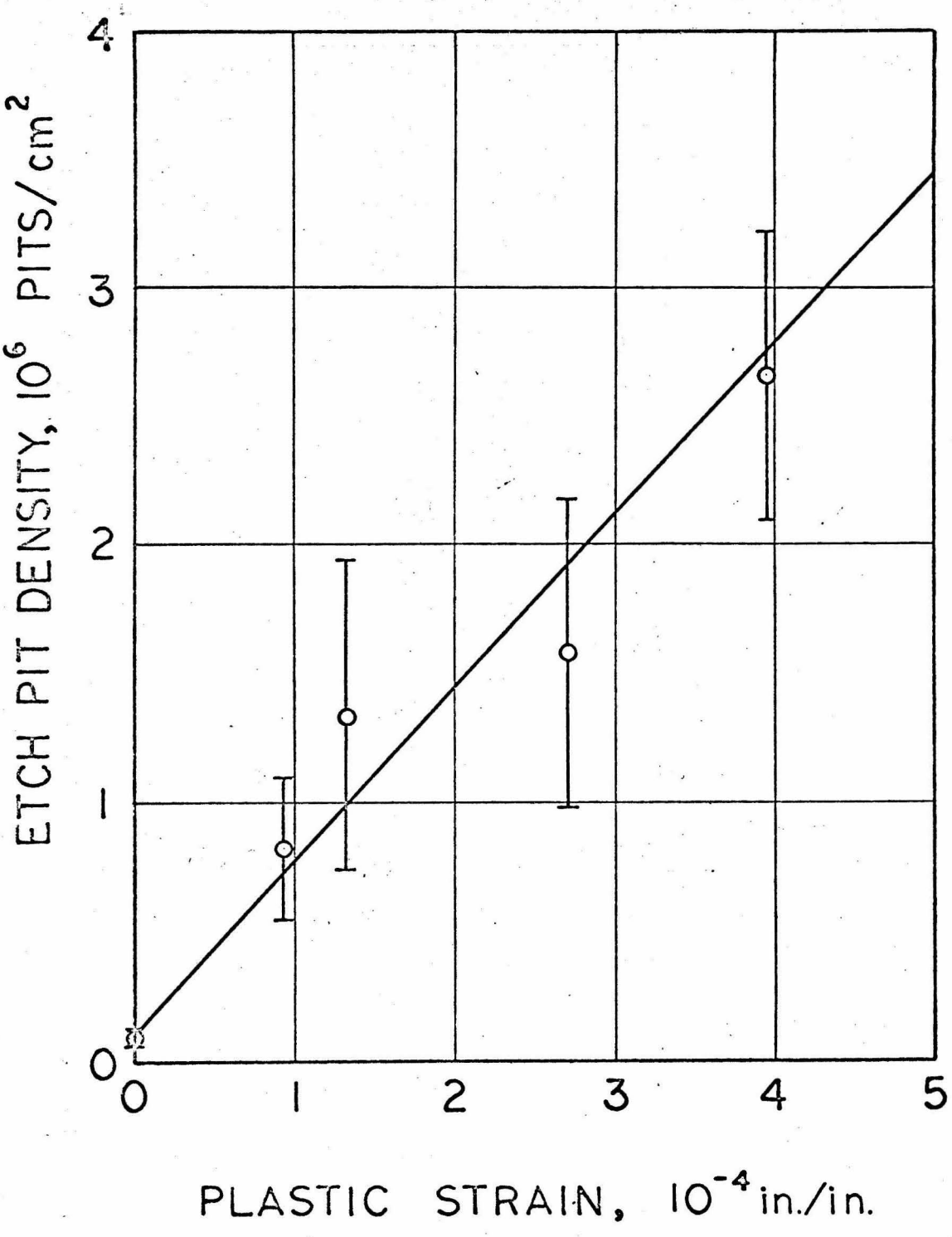

Fig. 4 Etch pit density on $(10\bar{1}0)$ prism planes vs. compressive strain along the [0001] hexagonal axis.

shear stress accompanying the change ($\Delta\tau << \tau$) . The data analysis gave an inverse strain-rate sensitivity of 720 ± 10 for both increasing and decreasing changes in strain-rate.

Pulse load tests were made at compressive stresses of from 390 to 2010 lb/in^2 for durations ranging from 51 x 10^{-3} to 33 sec. No significant generation or motion of dislocations from fresh scratches on $(10\bar{1}0)$ specimen surfaces was observed in these tests. Slip bands appeared on the $(10\bar{1}0)$ surfaces at compressive stresses in excess of 790 lb/in^2 whereas none were found between 390 and 690 lb/in^2 in pulses of 6.2 to 33 sec duration. Surfaces oriented at 5° to the (0001) were prepared on specimens containing slip bands, and these surfaces were etched to reveal dislocation intersections [9]. Slip bands were observed along traces of $\{ 1\bar{2}12 \}$ planes but not on traces of $\{ 10\bar{1}1 \}$ planes, indicating that the slip bands were of the second order and not the first order pyramidal system. Twinning occurred at stresses in excess of 2000 lb/in^2. The slip bands which formed in 31.4 sec at a compressive stress of 970 lb/in^2 (405 lb/in^2 resolved shear stress in the $\langle 1\bar{2}13 \rangle$ $\{ 1\bar{2}12 \}$ system) are shown in Fig. 5. Typically only two of the six possible $\{ 1\bar{2}12 \}$ slip plane traces are observed on the $(10\bar{1}0)$ surfaces as shown in Fig. 5. These slip plane traces make an angle of 28.3° with the [0001].

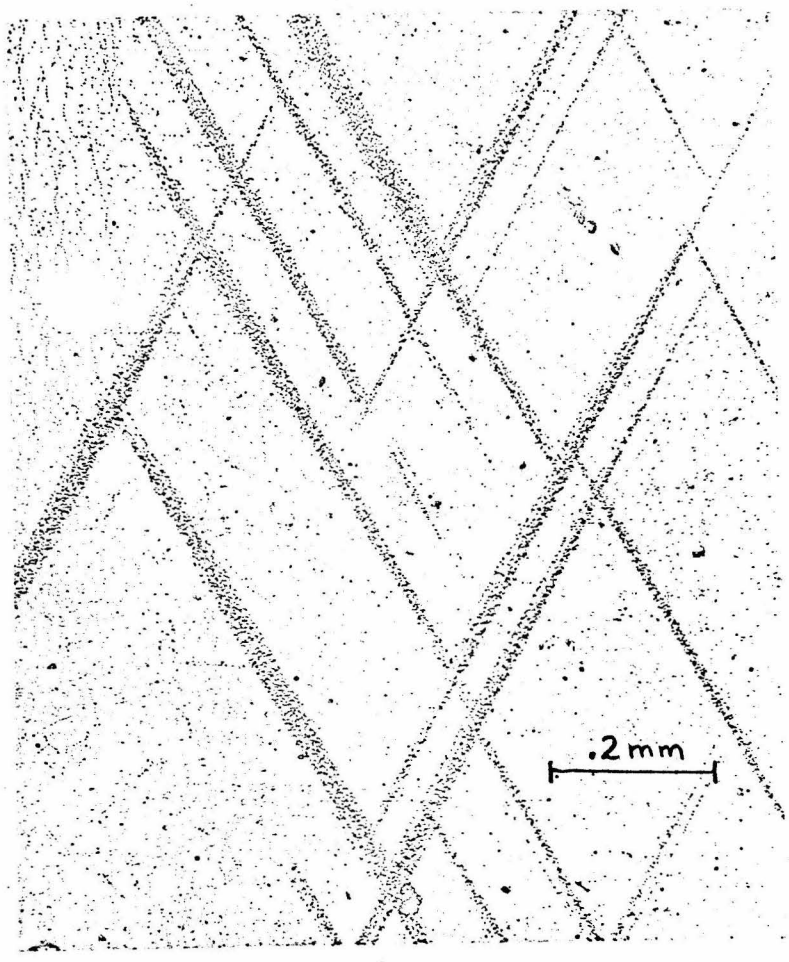

Fig. 5 Slip bands formed on a $(10\bar{1}0)$ surface in 31.4 sec at a compressive stress of 970 lb/in^2. [0001] axis is vertical.

The dislocation velocity was calculated from the longest length of new slip band produced at a given stress assuming that the leading dislocations moved one-half of the total slip band length during the duration of the stress pulse. This is equivalent to assuming that the dislocation sources are located on the surface at the center of the longest bands. The experimental data is shown in Fig. 6 plotted as log velocity vs. log resolved shear stress. The straight line drawn through the points corresponds to a power law relation of the form

$$v = v_o \, (\tau/\tau_o)^n \, , \qquad (2)$$

where v = dislocation velocity,

v_o = 1 in/sec,

n = 8.7,

τ_o = resolved shear stress of 870 lb/in^2 .

DISCUSSION

Pyramidal slip at room temperature occurs on the $\langle 1\bar{2}1\bar{3} \rangle$ $\{ 1\bar{2}12 \}$ system. The onset of pyramidal slip is associated with the formation of slip bands. The work hardening rate in c axis compression is much higher than that observed in basal slip [7]. This is in part due to the simultaneous operation of six intersecting slip systems, each equally

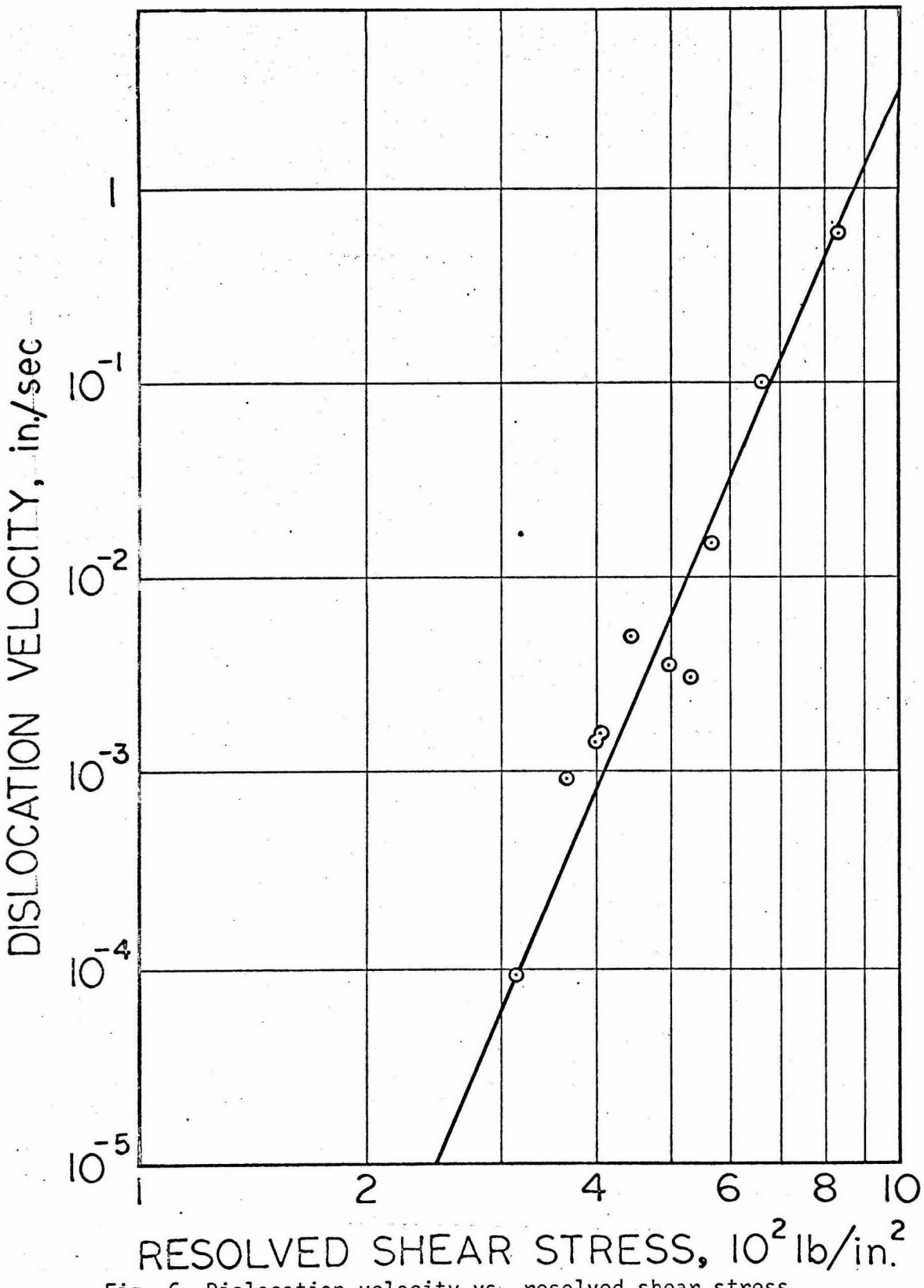

Fig. 6 Dislocation velocity vs. resolved shear stress.

stressed. The basal shear stress vs. shear strain curve exhibits only stage I deformation associated with easy glide. The stress-strain curve in c axis compression has no stage I or easy glide region. The slip bands observed on $(10\bar{1}0)$ planes cover the majority of the surface at a c axis strain of 10^{-4} in/in. The average density of etch pits on $(10\bar{1}0)$ surfaces increases linearly with strain up to 4×10^{-4} in/in. A considerable variation in etch pit density at a given strain is noted in different areas of the $(10\bar{1}0)$ surfaces. This is a result of the nonhomogeneous distribution of the slip bands.

The dislocation density increases with strain considerably faster in second order pyramidal slip than in basal slip (basal dislocation density is proportional to the 1/3 power of strain [7]). This is attributed to the relatively short slip distance of a pyramidal dislocation before cross slip takes place. Slip distances of the order of specimen dimensions were observed in basal slip with very little broadening of slip bands taking place before they extended across the specimen.

The appearance of the second order pyramidal slip bands on $(10\bar{1}0)$ surfaces is similar to that of slip bands in deformed crystals of lithium fluoride [10] where dislocation multiplication has been attributed to a multiple cross slip mechanism. Cross slip will be

likely in cases where screw dislocations are not extended into widely spaced partial dislocations and when a resolved shear stress occurs on the cross slip plane. Extensive cross slip of dislocations with $\frac{1}{3}\langle 1\bar{2}1\bar{3}\rangle$ Burgers vectors was observed in zinc by Price [3]. This most likely occurred on $\{10\bar{1}1\}$ or first order pyramidal planes because these planes are the only other low index planes that contain the $\langle 1\bar{2}1\bar{3}\rangle$ slip direction. In addition, Price observed large dipole trails and jogs on screw dislocations which were attributed to cross slip. In the c axis compression tests, the resolved shear stress on the first order pyramidal plane is equal to about 90 per cent of that on the second order pyramidal plane. Conditions are thus favorable for cross slip to occur and hence the conclusion is drawn that multiple cross slip is responsible for the nature of the observed slip bands.

The two slip band traces most frequently observed on the specimen prism surfaces correspond to $\{1\bar{2}12\}$ planes which make a normal intersection with the observation surface. Edge dislocations on these planes will lie perpendicular to the observation surface and screw dislocations will lie parallel to it. The dislocations observed in the direct mobility experiment are therefore most likely close to the edge orientation with a 1/3 $\langle 1\bar{2}1\bar{3}\rangle$ Burgers vector. The shape of a slip band appears to remain essentially constant, i.e. growth proceeds at a uniform rate in length and width.

The general absence of $\{ 1\bar{2}12 \}$ slip bands intersecting $(10\bar{1}0)$ surfaces with traces at 47.2° to the [0001] after pulse load tests was observed. Thus a definite preference appears to exist for the operation of surface sources which have a Burgers vector parallel to the surface. A surface step along the slip plane trace is not formed by the operation of these sources. The preference for the activity of sources with Burgers vectors parallel to the surface implies that the crystallographic orientation of the free surfaces of a tension or compression specimen could influence the observed plastic behavior.

Dislocation velocity in the second order pyramidal system has been observed to be influenced by the crystal substructure. Specimens prepared by acid machining, rather than by the spark erosion process used in this study, have significantly less substructure and show a significantly higher dislocation velocity at a given stress. This result is in qualitative agreement with the findings of Lavrent'yev et al. [5]. A quantitative study of this effect and the temperature dependence of dislocation velocity in the $\langle 1\bar{2}1\bar{3} \rangle \{ 1\bar{2}12 \}$ system is underway at this laboratory.

A comparison may be made of the inverse strain-rate sensitivity determined in the variable strain-rate test and the mobility exponent determined in the pulse load tests. The plastic strain-rate is related to the density of moving dislocations, ρ_m, and the average dislocation velocity, v, by

$$\dot{\gamma}_p = \rho_m \, b \, v \qquad (3)$$

where b is the Burgers vector of the dislocations in the active slip system. The inverse strain-rate sensitivity in Eq. 1 is thus

$$n' = \frac{\partial \, \ell n \, \rho_m}{\partial \, \ell n \, \tau} + \frac{\partial \, \ell n \, v}{\partial \, \ell n \, \tau} \, . \qquad (4)$$

The second term on the right hand side of Eq. 4 is the mobility exponent n of Eq. 2, which was found to be 8.7. The value of n' was determined to be 720. The difference must be attributed to the first term on the right hand side of Eq. 4. This indicates that there is a considerable change in the density of moving dislocation with a change in stress and the stress dependence of ρ_m is more important than the stress dependence of v as they affect the strain-rate sensitivity. The stress dependence of ρ_m has been neglected by some investigators when attempting to analyze the results of variable strain-rate tests.

CONCLUSIONS

(i) Zinc specimens prepared for this investigation deform by slip on the $\langle 1\bar{2}1\bar{3} \rangle$ { $1\bar{2}12$ } system at room temperature when subjected to

compressive stresses in excess of 790 lb/in^2 along [0001]. Slip is observed to be initially concentrated in slip bands which cover the specimen surfaces at a strain level of approximately 10^{-4} in/in.

(ii) The dislocation density increases linearly with strain in the [0001] direction between 10^{-4} and 4×10^{-4} in/in.

(iii) The velocity of edge dislocations in slip bands follows the relation $v = v_o (\tau/\tau_o)^n$, with $n = 8.7$, $\tau_o = 870$ lb/in^2 , $v_o = 1$ in/sec , and τ the resolved shear stress, lb/in^2.

(iv) The stress dependence of the moving dislocation density is considerably greater than the stress dependence of the dislocation velocity in $\langle 1\bar{2}1\bar{3} \rangle \{ 1\bar{2}12 \}$ slip.

(v) A preference exists for the formation of slip bands on $(10\bar{1}0)$ surfaces resulting from slip on the two systems with slip directions parallel to $(10\bar{1}0)$ surfaces. The four other slip systems which intersect $(10\bar{1}0)$ surfaces are seldom observed even though they are equally stressed.

ACKNOWLEDGEMENTS

The authors wish to express their appreciation to the U. S. Atomic Energy Commission for sponsorship of this work under Contract No. AT(04-3)-473 and to Professor D. S. Wood for his interest and advice during the course of this work. The assistance of J. L. Held in the testing and data analysis is gratefully acknowledged.

REFERENCES

1. K. H. Adams, T. Vreeland, Jr., and D. S. Wood, Mat. Sci. Eng., in press.

2. H. S. Rosenbaum, Acta Met., 9 (1961) 742.

3. P. B. Price, Phil. Mag., 5 (1960) 873.

4. A. A. Predvoditelev, G. V. Bushuyeva, and V. M. Stapanova. Fiz. Metal. Metalloved., 14 (1962) 687.

5. F. F. Lavrent'yev, O. P. Salita, and V. I. Startsev, Fiz. Metal. Metalloved., 21 (1966) 97.

6. E. J. Stofel and D. S. Wood, in D. C. Drucker and J. J. Gilman (eds.), Fracture of Solids, Gordon and Breach, New York, 1963, p. 521.

7. K. H. Adams and T. Vreeland, Jr., submitted to Trans. Met. Soc. AIME.

8. A. P. L. Turner, K. H. Adams, and T. Vreeland, Jr., Mat. Sci. Eng., 1 (1966) 70.

9. K. H. Adams, R. C. Blish and T. Vreeland, Jr., J. Appl. Phys., 37 (1966) 4291.

10. W. G. Johnston and J. J. Gilman, J. Appl. Phys., 31 (1960) 632.

LEGENDS TO FIGURES

Fig. 1 Compressive stress vs. compressive strain along [0001], 99.999% Zinc at room temperature.

Fig. 2 Typical areas of specimens strained in compression along [0001], $(10\bar{1}0)$ surface. (a) No strain, (b) 132 μ in/in, (c) 270 μ in/in, (d) 395 μ in/in. Lines indicate $[\bar{1}2\bar{1}0]$ direction, compression axis is vertical.

Fig. 3 An area showing slip bands on the six systems intersecting the $(10\bar{1}0)$ plane.

Fig. 4 Etch pit density on $(10\bar{1}0)$ prism planes vs. compressive strain along the [0001] hexagonal axis.

Fig. 5 Slip bands formed on a $(10\bar{1}0)$ surface in 31.4 sec at a compressive stress of 970 lb/in^2. [0001] axis is vertical.

Fig. 6 Dislocation velocity vs. resolved shear stress.